

# ChemComm

Chemical Communications

Accepted Manuscript

This article can be cited before page numbers have been issued, to do this please use: A. Juan, H. Sun, J. Qiao and J. Guo, *Chem. Commun.*, 2020, DOI: 10.1039/D0CC05910B.



This is an Accepted Manuscript, which has been through the Royal Society of Chemistry peer review process and has been accepted for publication.

Accepted Manuscripts are published online shortly after acceptance, before technical editing, formatting and proof reading. Using this free service, authors can make their results available to the community, in citable form, before we publish the edited article. We will replace this Accepted Manuscript with the edited and formatted Advance Article as soon as it is available.

You can find more information about Accepted Manuscripts in the [Information for Authors](#).

Please note that technical editing may introduce minor changes to the text and/or graphics, which may alter content. The journal's standard [Terms & Conditions](#) and the [Ethical guidelines](#) still apply. In no event shall the Royal Society of Chemistry be held responsible for any errors or omissions in this Accepted Manuscript or any consequences arising from the use of any information it contains.

## COMMUNICATION

**Near-infrared light-controlled circularly polarized luminescence of self-organized emissive helical superstructures assisted by upconversion nanoparticles**

Ao Juan†, Hao Sun†, Jinghui Qiao† and Jinbao Guo\*

Received 00th January 20xx,  
Accepted 00th January 20xx

DOI: 10.1039/x0xx00000x

**A near-infrared light-driven self-organized emissive helical superstructure was constructed by doping a new chiral fluorescent photoswitch and upconversion nanoparticles (UCNPs) into a nematic LC. The reversible switching of circularly polarized luminescence (CPL) can be achieved by modulating the power intensity of the 980 nm NIR excitation light.**

Chiroptical functional materials showing circularly polarized luminescence (CPL) have attracted much attention because of their attracting properties and promising potential for applications such as 3D displays, information encryption, optical sensors, and photoelectric devices.<sup>1-4</sup> The magnitude of circular polarization of CPL materials in the excited state is generally quantified by the luminescence dissymmetry factor ( $g_{em}$ ), which represents the ratio of the difference in intensity divided by the average total luminescence intensity:  $g_{em} = 2 \times (I_L - I_R)/(I_L + I_R)$  (1), where  $I_L$  and  $I_R$  are the intensities of the left and right circularly polarized emissions, respectively.<sup>3b</sup> To satisfy the requirement of practical applications, the development of novel CPL materials with high  $g_{em}$  values and sensitive to external stimuli is highly desirable.<sup>5</sup> Among the various kind of the developed CPL materials,<sup>6-22</sup> cholesteric liquid crystal (CLC) with a self-organized helical superstructure is an ideal matrix for developing strong CPL signals, high  $g_{em}$  values and tunable CPL responses.<sup>14-22</sup> Tunable CPL properties in CLC media by external stimuli such as temperature, light and electric field have been reported recently.<sup>15c,16,20-22</sup> As one of the most promising ones, phototunable CPL responses in a self-organized helical superstructure exhibit tunable optical characteristics and moderate  $g_{em}$  value, demonstrating great potentials for real applications. Very recently, the switchable CPL intensity and helical handedness in the CLCs media with luminescent helical superstructure have been reported by our group.<sup>21,22</sup> In these two cases, ultraviolet (UV) light and visible light have been employed to trigger the photoreaction

process of the chiral fluorescent photoswitches used in the systems. In fact, using near-infrared (NIR) light in many fields is urgently needed compared to the used UV or visible light due to its numerous advantages, such as deep penetration, precise control with low interference. Thus, it is highly desirable to develop NIR-light responsive CLCs with tunable CPL signals.

In this work, we report the first example of 980 nm NIR-light-triggered reversible tuning of CPL and photoluminescence (PL) in the CLC with a self-organized emissive helical superstructure loaded with upconversion nanoparticles (UCNPs). As is well known, UCNPs can convert near-infrared light into UV light or visible light, thereby triggering the photochemical reaction of the photoresponsive LC materials.<sup>23</sup> As shown in Fig. 1, the doped core-shell-shell NaYF<sub>4</sub>-based UCNPs in the system can change the emitting light when the power density of 980 nm NIR light is increased or decreased. On one hand, the dominant 520 nm green light derived from the UCNPs at low power densities can trigger *trans* to *cis* photoisomerization of the novel chiral fluorescent photoswitch doped in the CLCs system, yielding that a sharply decrease of both PL and CPL intensity of the CLC shown in Fig. 1. On the other hand, the reverse process happened when induced by the 365 nm UV and 450 nm blue emissions upon irradiation by the 980 nm NIR laser at high power density. This "remote-control" photoswitching using NIR light allows us to achieve optically-rewritable PL pattern as well as CPL pattern with a moderate resolution. This technology offers a highly convenient method to effectively switch CPL and PL in an emissive CLC using a single NIR-light source.

A new chiral fluorescent switch **6** is used to induce the formation of photoresponsive self-assembly helical superstructure shown in Fig. 1. The switch **6** was synthesized following a procedure described in our previous reports.<sup>21,24</sup> The detailed description of the synthetic procedures (Scheme S1) and structural characterizations are provided in Supporting Information. The initial state and variation of CD spectrum of final product switch **6** is shown in Fig. S1. The optimized ground-state geometries of *trans* and *cis* isomers of switch **6** are calculated by Gaussian 09 using density functional theory (DFT) at B3LYP/6-31G(d) level, in which *trans* isomers are 3.99 kcal/mol lower than *cis* isomers (Fig. S2). A low energy gap between *trans* and

Key Laboratory of Carbon Fibers and Functional Polymers, Ministry of Education, and College of Materials Science and Engineering, Beijing University of Chemical Technology, Beijing 100029, China. E-mail: [guojb@mail.buct.edu.cn](mailto:guojb@mail.buct.edu.cn)

†These three authors contributed equally to this work.

Electronic Supplementary Information (ESI) available: [details of any supplementary information available should be included here]. See DOI: 10.1039/x0xx00000x

*cis* isomers is beneficial to inversion of C=C configuration, which promotes the conversion of *trans/cis* photoisomerization of switch **6**. As shown in Fig. S3, the *trans* to *cis* photoisomerization of switch **6** is effectively triggered by 520 nm green light, and the reverse isomerization occurs upon irradiation by 365 nm UV light or 450 nm blue light. In fact, the experimental result is in well agreement with the theoretical analysis (Table S1). PL spectra of switch **6** shows an emission peak at around 580 nm shown in Fig. S4, which exhibits a large intensity variation between initial state and photostationary state of 520 nm (PSS<sub>520</sub>). And the PL intensity partly recovers at PSS<sub>450</sub> and PSS<sub>365</sub> upon 365 nm light or 450 nm light irradiations because of the *cis* to *trans* isomerization. Furthermore, the photoisomerization conversions could be verified based on the quantitative analysis of characteristic <sup>1</sup>H-NMR peaks (Fig. S5 of supporting information). All the above observations reveal that the photoswitchable reversible *trans/cis* photoisomerization of switch **6** happens with moderate conversions. In addition, the photo-responsive behavior of switch **6** in a nematic LC host was demonstrated by the Grandjean-Cano method (Fig. S6 and Fig. S7), in which the weight ratio of switch **6** to SLC1717 was 0.25:99.75. On the basis of calculated helical twisted power (HTP) values in different photostationary states, it is clearly observed that the HTP values obviously decreases from initial state to PSS<sub>520</sub> while it can partly recover separately irradiated by 450 nm blue light or 365 nm UV light.

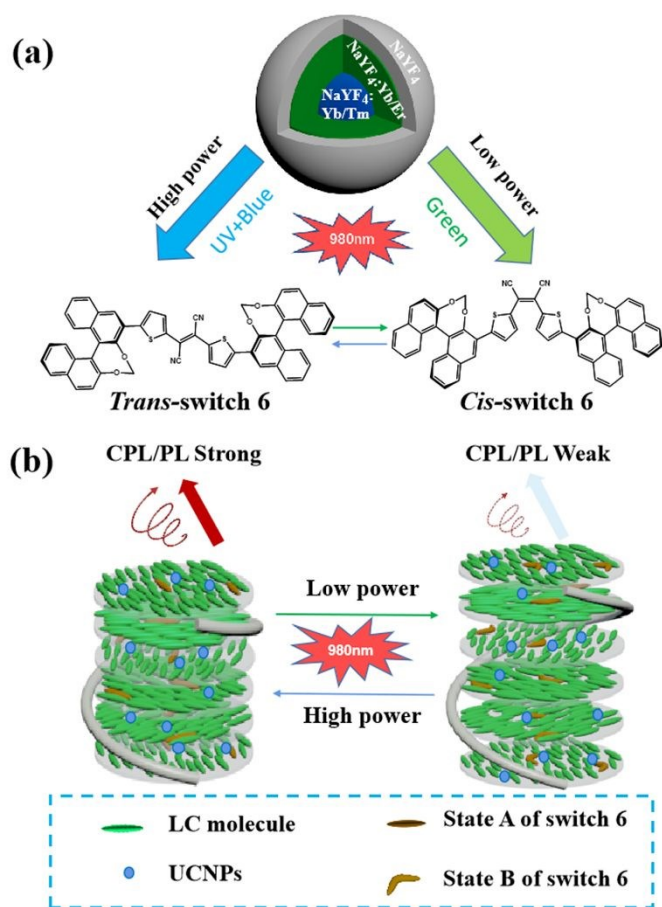


**Fig. 1** (a) Schematic diagram of the photoisomerization of switch **6**, which is triggered in a control process using 980 nm NIR laser light;

(b) Schematic of reversible tuning of self-organized luminescent helical superstructures with switch **6** and UCNP upon irradiation of 980 nm NIR laser at different power densities.

The used NaYF<sub>4</sub>-based UCNP with core-shell-shell nanostructures was prepared using a three-step solvothermal method according to the detailed description in the supporting information. To achieve a better selective upconversion emission from NIR light to UV light/blue light and green light in this study,  $\beta$ -NaYF<sub>4</sub>, 0.5 mol% Tm<sup>3+</sup>, 30 mol % Yb<sup>3+</sup> cores were coated with a  $\beta$ -NaYF<sub>4</sub>, 2 mol % Er<sup>3+</sup>, 15 mol % Yb<sup>3+</sup> followed by an undoped  $\beta$ -NaYF<sub>4</sub> shell. The nanoparticles were easily verified to hexagonal-phase NaYF<sub>4</sub> based on powder X-ray diffraction data as shown in Fig. S8. Transmission electron microscopy (TEM) images of the UCNP (Fig. S9) shows that they possess uniform hexagonal shapes. As shown in Fig. 2a, the 520 nm green emission dominates the spectrum at low power density (0.15 W/mm<sup>2</sup>), while the 365 nm UV and 450 nm blue emission from the UCNP are greatly increased at high power density (3.0 W/mm<sup>2</sup>) shown in Fig. 2b. As shown in Fig. S10, around 520 nm green emissions (<sup>4</sup>H<sub>11/2</sub>→<sup>4</sup>I<sub>15/2</sub> transition) generated from the Yb<sub>3+</sub>→Er<sub>3+</sub> energy transfer process at low power density of 980 nm laser light overlap with the absorption bands corresponding to *trans* form of switch **6**, in which this emission may be utilized to trigger the *trans* to *cis* photoisomerization of the photoswitch. While 365 nm UV and 450 nm blue emissions (<sup>1</sup>D<sub>2</sub>→<sup>3</sup>H<sub>6</sub> and <sup>1</sup>D<sub>2</sub>→<sup>3</sup>F<sub>4</sub> transitions) derived from Yb<sub>3+</sub>→Tm<sub>3+</sub> energy transfer process could be obtained in a higher excitation power density of 980 nm laser light, thus making it possible for the emitted UV and blue light of UCNP to trigger its *cis* to *trans* isomerization.

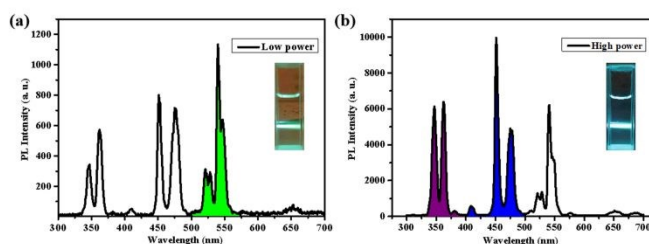


**Fig. 2** Emission spectra of UCNP (60 µg/mL) in dichloromethane at room temperature upon irradiation with 980 nm NIR laser (a) at low power density (0.15 W/mm<sup>2</sup>) and (b) at high power density (3.0 W/mm<sup>2</sup>).

Fig. 3a and 3b show the changes in the UV-vis spectra and PL spectra of switch **6** (50 µg/mL) and UCNP (2.0 mg/mL) in dichloromethane respectively upon irradiation with 980 nm NIR laser. When irradiated by 980 nm NIR laser at low power density (0.15 W/mm<sup>2</sup>) for 30 min, the absorption band at around 490 nm shifts to around 450 nm with decrease in intensity due to *trans* to *cis* photoisomerization of switch **6**. Upon 980 nm NIR laser at high power density (3.0 W/mm<sup>2</sup>) for 10 min, the absorption band centered around 450 nm, corresponding to  $\pi$ - $\pi^*$  transition of *cis* isomer, red shifts with concomitant increase in its intensity till the PSS is reached due to *cis* to *trans* isomerization. Meanwhile, a large PL intensity variation could be clearly observed when *trans* to *cis* photoisomerization of switch **6** happened. The PL intensity recovers to an intermediate level upon *cis* to *trans* isomerization. All above observations suggest that the photoisomerization properties of

switch **6** can be effectively modulated by 980 nm NIR laser light, and the reversible *trans* to *cis* and *cis* to *trans* photoisomerization process can be induced only by modulating the excitation power density of the 980 nm laser light.

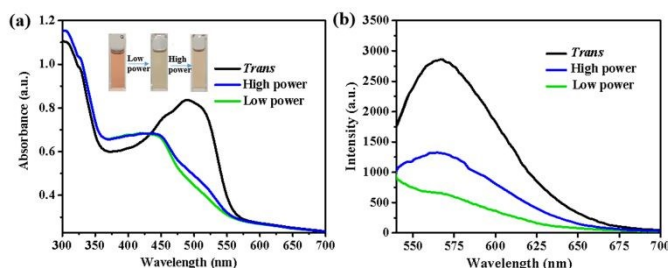


**Fig. 3** Changes in the UV-vis spectra (a) and PL spectrum (b) of switch **6** (50  $\mu\text{g}/\text{mL}$ ) and UCNPs (2.0  $\text{mg}/\text{mL}$ ) in dichloromethane at room temperature upon irradiation with 980 nm NIR laser at high power density (3.0  $\text{W}/\text{mm}^2$ ) and upon irradiation with 980 nm NIR laser at low power density (0.15  $\text{W}/\text{mm}^2$ ).

The phototunable PL and CPL behaviors of the CLC sample doped with 1.0 wt% of switch **6** and 0.5 wt% UCNPs into SLC1717 were recorded. As shown in Fig. 4a, the PL intensity of the CLC sample drastically drops to a low level upon 980 nm NIR laser at low power density (0.15  $\text{W}/\text{mm}^2$ ) for 10 min. When exposed to 980 nm NIR laser at high power density (3.0  $\text{W}/\text{mm}^2$ ) for 1.0 min, the PL intensity increased. We further investigated the changes of CPL spectra in the CLC sample upon light irradiation shown in Fig. 4b and Fig. S11, the phototunable CPL could also be observed. The CPL signal decreased upon low-power 980 nm NIR light irradiation; while the intensity of the CPL signal partly recovered when exposed to high-power 980 nm NIR laser light. The tendency of this variation was further verified by CD spectrum characterization shown in Fig. 4c. Notably, the  $g_{\text{em}}$  absolute value at the initial state could be close to 0.49, which is ascribed to the self-organized helical structure of the CLCs. Meanwhile, the  $g_{\text{em}}$  absolute value also undergoes a decrease first and then a slight increase during the light irradiations as shown in Fig. 4d. And a dynamic reversible switching of the CPL signal and  $g_{\text{em}}$  value between PSS<sub>980-l</sub> and PSS<sub>980-h</sub> could be achieved upon 980 nm laser light irradiations with alternate low power and high power. All the above observations fully demonstrate that the PL as well as CPL signal of the CLC could be reversibly switched upon the 980 nm NIR laser at low power density and high power density.

A schematic of illuminating the PL/CPL dual-mode rewritable optical storage device is shown in Fig. 5a, here a beam expander is used in the system to modulate the emission intensity of 980 nm laser light. The fluorescent dot array with modest contrast can be written on the cell using a photomask upon 980 nm NIR laser at high power density irradiation and the information can be erased by 980 nm NIR laser at low power density. In addition, the information or data can be easily and rapidly written without physical contact and photomask using the above equipment. As shown in Fig. 5b, a high-contrast PL pattern could be written, erased and rewritten. Meanwhile, due to the strong/weak switching of CPL signal, a CPL pattern featuring S/W encrypted mode was also obtained as demonstrated in Fig. 5a. Based on the spectacular feature of the photo-responsive reversible dynamic tuning, a novel integrated combinational dual-mode device capable of showing both PL and

CPL-encryption information through changing the corresponding 980 nm laser input signals was successfully established.

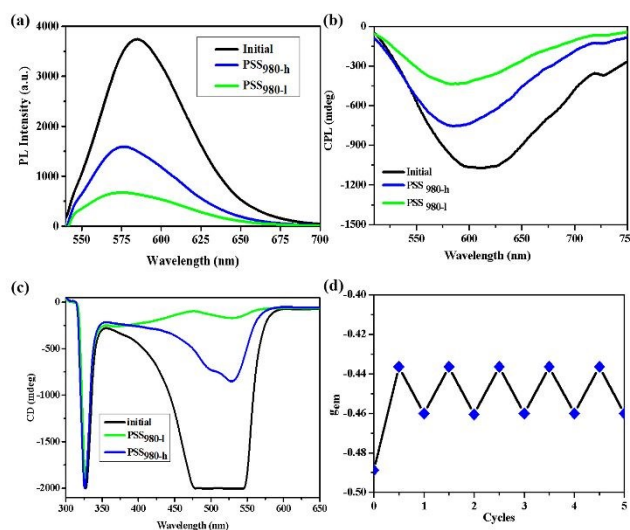


**Fig. 4** (a) PL spectra and (b) CPL spectra of photo-responsive CLC doping 1.0 wt% of switch **6** and 0.5 wt% UCNPs into SLC1717 tuned by 980 nm NIR laser at high power density (3.0  $\text{W}/\text{mm}^2$ ) and at low power density (0.15  $\text{W}/\text{mm}^2$ ). (c) CD spectra of photo-responsive CLC doping 0.2 wt% of switch **6** and 0.1 wt% UCNPs; Note that: considering the testing range of CD spectrum, the doped switch **6** and UCNPs were diluted by 5 times in the configured CLC mixture. (d) Fatigue resistance test of variation of  $g_{\text{em}}$  at 605 nm upon alternate irradiations with 980 nm NIR laser at high power density and at low power density.

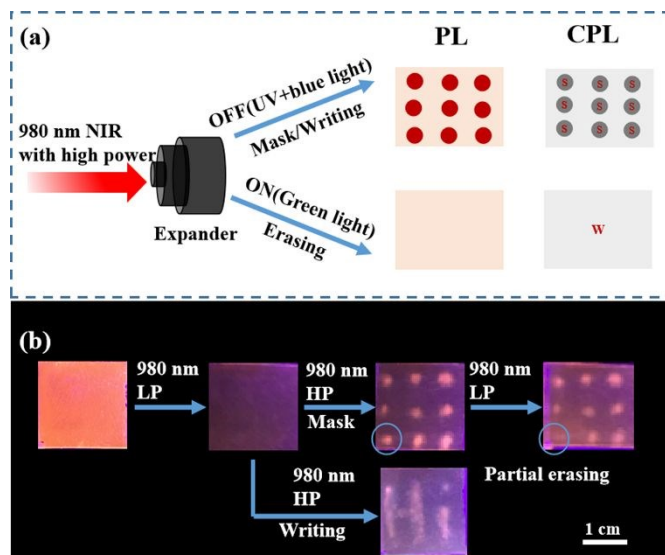


**Fig. 5** (a) Schematic diagram of illuminating the PL/CPL dual-mode rewritable optical storage; (b) Real images of PL/CPL dual-mode patterns (note that S: strong CPL signal; W: weak CPL signal).

In summary, we proposed a NIR-light-controlled CPL and PL in a self-organized emissive helical superstructure fabricated by doping a new chiral fluorescent photoswitch and UCNPs into a nematic LC host. The consequent CPL as well as PL were found to be reversibly

tuned simply by varying the excitation power density of the 980 nm NIR laser. Furthermore, the NIR-light-triggered PL/CPL dual-mode patterns in the single thin films for the rewritable optical storage devices were successfully established, and writing/erasing process was demonstrated by modulating the NIR light power density. This work offers a convenient method to regulate the self-organized emissive helical superstructures and their dynamic CPL and PL for photonic applications.

We acknowledge the supports from National Natural Science Foundation of China (Grant Nos. 51773009 and 52073017). This work is supported by High Performance Computing Platform of Beijing University of Chemical Technology.

### Conflicts of interest

There are no conflicts to declare.

### Notes and references

- J. M. Han, S. Guo, H. Lu, S. J. Liu and Q. Zhao, *Adv. Opt. Mater.*, 2018, **6**, 1800538.
- (a) F. Pop, N. Zigon and N. Avarvari, *Chem. Rev.*, 2019, **119**, 8435–8478; (b) A. Nitti and D. Pasini, *Adv. Mater.*, 2020, **32**, 1908021.
- (a) T. H. Zhao, J. L. Han, P. F. Duan and M. H. Liu, *Acc. Chem. Res.*, 2020, **53**, 1279–1292; (b) Y. T. Sang, J. L. Han, T. H. Zhao, P. F. Duan and M. H. Liu, *Adv. Mater.*, 2019, **31**, 1900110; (c) F. Zinna, G. Albano, A. Taddeucci, T. Colli, L. A. Aronica, G. Pescitelli, L. D. Bari, *Adv. Mater.*, 2020, **32**, 2002575.
- J. Roose, B. Z. Tang and K. S. Wong, *Small*, 2016, **12**, 6495–6512.
- (a) Y. Gao, C. Ren, X. D. Lin and T. C. He, *Front. Chem.*, 2020, **8**, 458; (b) J. L. Ma, Q. Peng, C. H. Zhao, *Chem. Eur. J.*, 2019, **25**, 15441–15454; (c) D. Zheng, L. Zheng, C. Y. Yu, Y. L. Zhan, Y. Wang, H. Jiang, *Org. Lett.*, 2019, **21**, 2555–2559; (d) D. Zheng, C. Y. Yu, L. Zheng, Y. L. Zhan, H. Jiang, *Chin. Chem. Lett.*, 2020, **31**, 673–676.
- (a) K. Takaishi, M. Yasui and T. Ema, *J. Am. Chem. Soc.*, 2018, **140**, 5334–5338; (b) K. Takaishi, K. Iwachido and T. Ema, *J. Am. Chem. Soc.*, 2020, **142**, 1774–1779.
- A. H. G. David, R. Casares, J. M. Cuerva, A. G. Campaña and V. Blanco, *J. Am. Chem. Soc.*, 2019, **141**(45), 18064–18074.
- F. Zinna, U. Giovanella and L. D. Bari, *Adv. Mater.*, 2015, **27**, 1791–1795.
- (a) D. Yang, P. F. Duan, L. Zhang and M. H. Liu, *Nat. Commun.*, 2017, **8**, 15727–15736; (b) Y. H. Shi, P. F. Duan, S. W. Huo, Y. G. Li and M. H. Liu, *Adv. Mater.*, 2018, **30**, 1705011; (c) Q. X. Jin, S. X. Chen, Y. T. Sang, H. Q. Guo, S. Z. Dong, J. L. Han, W. J. Chen, X. F. Yang, F. Li and P. F. Duan, *Chem. Commun.*, 2019, **55**, 6583–6586; (d) J. L. Han, D. Yang, X. Jin, Y. Q. Jiang, M. H. Liu and P. F. Duan, *Angew. Chem. Int. Ed.*, 2019, **58**, 7013–7019.
- (a) W.-B. Lin, D.-Q. He, H.-Y. Lu, Z.-Q. Hu and C.-F. Chen, *Chem. Commun.*, 2020, **56**, 1863–1866; (b) M. Li, C. Zhang, L. Fang, L. Shi, Z. Y. Tang, H.-Y. Lu and C.-F. Chen, *ACS Appl. Mater. Interfaces*, 2018, **10**, 8225–8230; (c) F. Wang, W. Ji, P. Yang and C. L. Feng, *ACS Nano*, 2019, **13**, 7281–7290.
- B.-C. Kim, H.-J. Choi, J.-J. Lee, F. Araoka and S.-W. Choi, *Adv. Funct. Mater.*, 2019, **29**, 1903246.
- Q. Jiang, X. H. Xu, P.-A. Yin, K. Ma, Y. G. Zhen, P. F. Duan, Q. Peng, W.-Q. Chen and B. Q. Ding, *J. Am. Chem. Soc.*, 2019, **141**, 9490–9494.
- (a) B. Zhao, H. L. Yu, K. Pan, Z. A. Tan and J. P. Deng, *ACS Nano*, 2020, **14**(3), 3208–3218; (b) B. Zhao, X. B. Gao, N. Lu and J. P. Deng, *Adv. Opt. Mater.*, 2018, **6**, 2000858.
- (a) H. Z. Zheng, W. R. Li, W. Li, X. J. Wang, Z. Y. Tang, S. X.-A. Zhang and Y. Xu, *Adv. Mater.*, 2018, **30**, 1705948; (b) H. L. Yu, B. Zhao, J. B. Guo, K. Pan and J. P. Deng, *J. Mater. Chem. C*, 2020, **8**, 1459–1465.
- (a) X. J. Li, Q. Li, Y. X. Wang, Y. W. Quan, D. Z. Chen and Y. X. Cheng, *Chem. Eur. J.*, 2018, **24**, 12607–12612; (b) X. H. Gao, X. J. Qin, X. F. Yang, Y. G. Li and P. F. Duan, *Chem. Commun.*, 2019, **55**, 5914–5917; (c) X. J. Li, W. R. Hu, Y. X. Wang, Y. W. Quan and Y. X. Cheng, *Chem. Commun.*, 2019, **55**, 5179–5182; (d) Y. Li, K. R. Liu, X. J. Li, Y. W. Quan and Y. X. Cheng, *Chem. Commun.*, 2020, **56**, 1117–1120.
- (a) B. A. San Jose, J. L. Yan and K. Akagi, *Angew. Chem. Int. Ed.*, 2014, **53**, 10641–10644; (b) J. L. Yan, F. Ota, B. A. San Jose and K. Akagi, *Adv. Funct. Mater.*, 2017, **27**, 1604529.
- C. T. Wang, K. Q. Chen, P. Xu, F. Yeung, H. S. Kwok and G. J. Li, *Adv. Funct. Mater.*, 2019, **29**, 1903155.
- X. F. Yang, M. H. Zhou, Y. F. Wang and P. F. Duan, *Adv. Mater.*, 2020, **32**, 2000820.
- S. Y. Lin, H. Sun, J. H. Qiao, X. K. Ding and J. B. Guo, *Adv. Opt. Mater.*, 2020, **8**, 2000107.
- A. Bobrovsky, K. Mochalov, V. Oleinikov, A. Sukhanova, A. Prudnikau, M. Artemyev, V. Shibaev and I. Nabiev, *Adv. Mater.*, 2012, **24**, 6216–6222.
- J. T. Li, H. K. Bisoyi, S. Y. Lin, J. B. Guo and Q. Li, *Angew. Chem. Int. Ed.*, 2019, **58**, 16052–16056.
- J. H. Qiao, S. Y. Lin, J. T. Li, J. J. Tian and J. B. Guo, *Chem. Commun.*, 2019, **55**, 14590–14593.
- (a) S. Wu and H.-J. Butt, *Adv. Mater.*, 2016, **28**, 1208–1226; (b) L. Wang, H. Dong, Y. N. Li, C. M. Xue, L.-D. Sun, C.-H. Yan and Q. Li, *J. Am. Chem. Soc.*, 2014, **136**, 4480–4483; (c) L. Wang, H. Dong, Y. N. Li, R. Liu, Y.-F. Wang, H. K. Bisoyi, L.-D. Sun, C.-H. Yan and Q. Li, *Adv. Mater.*, 2015, **27**, 2065–2069; (d) W. Wu, L. M. Yao, T. S. Yang, R. Y. Yin, F. Y. Li and Y. L. Yu, *J. Am. Chem. Soc.*, 2011, **133**, 15810–15813.
- (a) J. T. Li, H. K. Bisoyi, J. J. Tian, J. B. Guo and Q. Li, *Adv. Mater.*, 2019, **31**, 1807751; (b) J. T. Li, Z. W. Zhang, J. J. Tian, G. Q. Li, J. Wei and J. B. Guo, *Adv. Opt. Mater.*, 2017, **5**, 1700014. (c) J. J. Tian, Y. R. He, J. T. Li, J. Wei, G. Q. Li and J. B. Guo, *Adv. Opt. Mater.*, 2018, **6**, 1701337; (d) S. Y. Lin, J. T. Li, H. K. Bisoyi, A. Juan, J. B. Guo and Q. Li, *ChemPhotoChem*, 2019, **3**, 480–486.